IEEE Photonics Journal
An IEEE Photonics Society Publication

Open Access

Dynamic Fano Resonance in Thin Fiber Taper Coupled Cylindrical Microcavity

Volume 8, Number 6, December 2016

Yadong Miao
Yunchong Peng
Yu Xiang
Mi Li
Yu Lu
Yuejiang Song

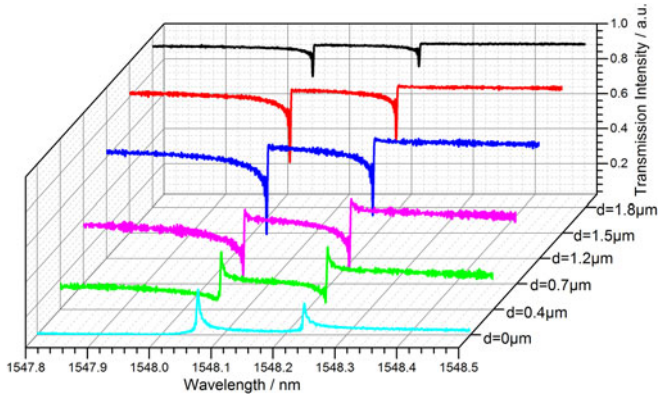

DOI: 10.1109/JPHOT.2016.2630316
1943-0655 © 2016 IEEE

IEEE photonics SOCIETY

IEEE

Dynamic Fano Resonance in Thin Fiber Taper Coupled Cylindrical Microcavity

Yadong Miao, Yunchong Peng, Yu Xiang, Mi Li, Yu Lu, and Yuejiang Song

Institute of Optical Communication Engineering, Nanjing University, Jiangsu 210009, China

DOI:10.1109/JPHOT.2016.2630316

Manuscript received October 11, 2016; revised November 10, 2016; accepted November 14, 2016. Date of publication November 17, 2016; date of current version December 9, 2016. This work was supported by the National Science Foundation of China under Grant 60907022 and Grant 41427801.
Corresponding author: Y. Song (e-mail: yjsong@nju.edu.cn).

Abstract: Fano resonance results from interference between a background and a resonant scattering, which produces the asymmetrical lineshape. A cylindrical microcavity naturally possesses localized whispering gallery mode (WGM) and delocalized radiation mode, and a thin fiber taper can excite these two modes simultaneously. The localized WGM can interfere with the weak delocalized background to generate Fano resonance in the thin fiber taper coupled cylindrical microcavity. In addition, the Fano parameter can be adjusted by changing the gap between fiber taper and microcylinder cavity or the coupling diameter of fiber taper. The experimental results agree well with the quantum scattering theory.

Index Terms: Microcavity, Fano resonance, radiation mode, whispering gallery mode (WGM), thin fiber taper.

1. Introduction

In atomic physics, Fano resonance, behaving like electromagnetically induced transparency (EIT), originates from quantum interference between a discrete excited state of an atom and a continuum with the same energy level [1], [2]. Reflected in the realm of classical optics [1], [3], it is the result of destructive interference between two scattering amplitudes: one as background process and the other as resonant process, respectively. The phase and magnitude experience dramatic changes at Fano resonance and any systematic or outer changes will lead to deformation of Fano lineshapes [4]–[6]. This unique property makes it possess many potential applications [7]–[9], including biochemical sensing, optical switch, slow light, etc. Fano resonance has been observed in many systems, including photonic crystal, semiconductor systems [10], plasmonic nanostructures [11], and optical resonators [12], [13]. Due to its high quality factor and small mode volume [14], whispering gallery mode (WGM) microcavities have attracted many researchers to study Fano resonance.

In whispering gallery mode microcavity, previous researchers can excite Fano resonance in three different mechanisms. First, Fano resonance is generated when a high-quality factor (Q) mode and a low-quality factor mode interfere. It can be observed in two directly coupled WGM microcavities, indirectly coupled WGM microcavities [3], or a single WGM microcavity side-coupled to a fiber taper [13], [15]. Secondly, Fano resonance is generated when a high Q mode and continuous chaos interfere with each other [16], [17]. Free-space laser beam focuses on the edge of deformed microtoroid and excites both high Q mode and chaotic mode. The interference between them

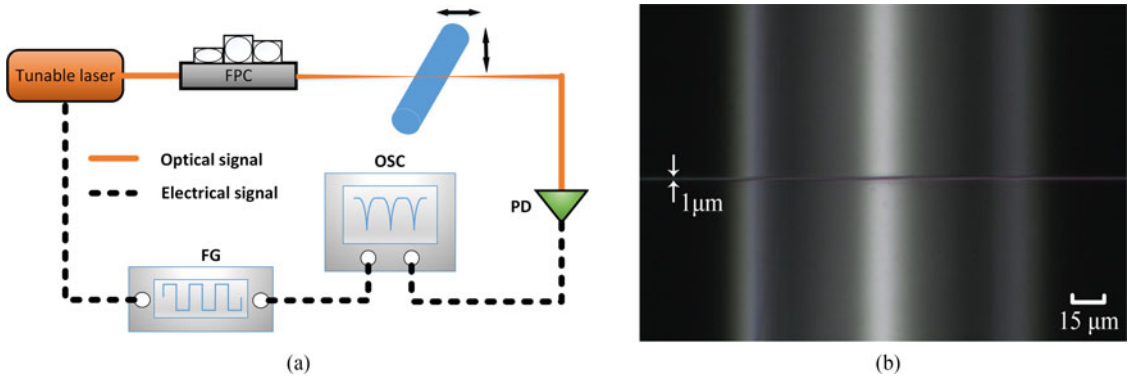

Fig. 1. (a) Schematic illustration of experimental setup. FPC: fiber polarization controller, PD: photodetector, OSC: oscilloscope, FG: function generator. (b) Micrograph of taper-microcylinder coupling system.

leads to the transmission spectrum evolving from resonant peak to Fano lineshape and then to resonant dip. Third, by dynamically adjusting intracavitary gain (or loss) or coupling strength, sharp asymmetric Fano lineshapes will be excited in the transmission spectrum. To accomplish it, pump method and multi-cavity coupling are two main approaches [7], [12], [18].

In this paper, we report the evolution of Fano resonance in thin fiber taper coupled cylindrical microcavity. Different from the enclosed microcavity, cylindrical microcavity possesses both localized WGM and delocalized radiation mode. This radiation mode is utilized to produce the continuous background for Fano resonance. When thin fiber taper excites both modes, the localized WGM coupled out of microcavity will interfere with the weak delocalized transmission background to generate Fano resonance. In addition, the Fano parameter can be dynamically adjusted by changing the distance gap between fiber taper and the microcavity or varying the coupling diameter of the fiber taper. The lineshape in the transmission spectrum transforms from resonant dip to asymmetrical Fano resonance and then, ultimately, to EIT-like resonant peak.

2. Experimental and Theoretical Analysis

The schematic setup of thin fiber taper coupled microcylinder and the microscope image of the coupled microcavity are shown in Fig. 1(a) and (b), respectively. As shown in Fig. 1(a), the tunable laser is injected into the fiber and then coupled into the cylindrical microcavity by fiber taper. The polarization controller is used to adjust the polarization of the light coupling into the cavity. The output light from fiber taper coupled microcavity system is detected by a PD, and the electrical signal is measured by an oscilloscope. The cylindrical microcavity is put on a precise 3-axis motorized stage and can be moved vertically or horizontally with resolution of 20 nm. Thus, the gap between the taper and the microcavity or the coupling diameter of the taper can be tuned precisely in the experiment.

In our experiment, cylindrical microcavity with diameter 125 μm is prepared by directly stripping the polymer coating of SM-28 fiber and fiber taper is fabricated by heating and stretching the bare fiber into a tight thread with waist diameter of $\sim$1 μm. The fabricated thin taper has low loss, typically less than 0.2 dB. Compared with other similar experiments, the fiber taper used in this experiment is the taper with thin diameter ($\sim$1 μm) and not the taper with large diameter. In a fiber taper coupled microcavity, fiber taper can not only excite but extract the optical field in the microcavity simultaneously. At the coupling junction, input light in fiber taper is divided into two parts, one part coupled into and then out of the microcavity as the discrete resonant mode and the other directly transmitted as the continuous background. When these two parts meet and interfere with each other in the fiber taper, Fano resonance can be generated if they have comparable amplitudes. Unlike the enclosed microcavity, such as microsphere or microtoroid, cylindrical microcavity is a type of

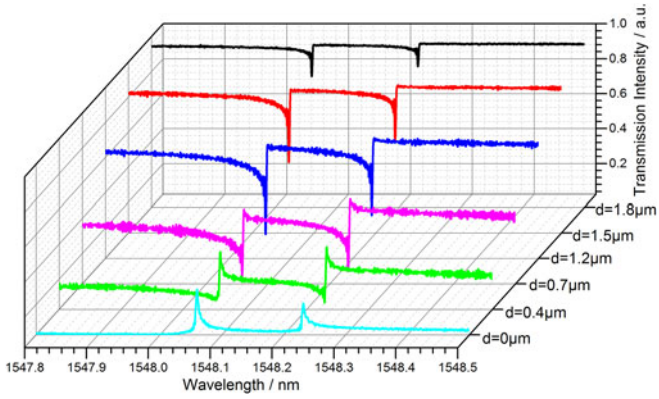

Fig. 2. Transmission spectra with the different gap d varying from 1.8 μm to 0 μm. All traces are normalized to the intensity without coupling between the taper and the microcylinder.

special microcavity because it naturally possesses both localized WGMs and delocalized radiation modes. WGM is localized in the transverse plane to the cylinder axis, while the delocalized radiation mode will experience total internal reflection and radiate out along the cylinder axis eventually [19], [20]. In the practical coupling experiment, the proper diameter of fiber taper should be chosen and the desired mode can be efficiently excited by approximate phase matching [21]. Generally, the low order localized WGM has larger mode index than the delocalized radiation mode in the microcylinder cavity. When the coupling diameter of fiber taper is large sufficiently, WGM can be excited efficiently while radiation mode is almost not excited in the cylinder due to its high mode index of large fiber taper. In this condition, the insertion loss of the large fiber taper coupled microcylinder is low and the intensity of transmitted background is high, but when the coupling diameter of fiber taper is thin ($\sim$1 μm), its mode index will be small and the radiation mode can be excited efficiently. The insertion loss of thin fiber taper coupled cylindrical microcavity may be very high and dominated by the coupling loss from fiber taper mode to the radiation mode. Thus, the transmitted background of thin fiber taper coupled microcylinder is relatively low in this condition.

In our first experiment, the coupling diameter of fiber taper is kept as thin as $\sim$1 μm, but the gap between fiber taper and microcylinder is dynamically adjusted. As we vertically adjust the gap, the transmission spectra are measured and shown in Fig. 2. During the gap adjustment, the background intensity decreases with the gap dramatically, also the lineshapes of transmission spectra transform from resonant dip to Fano resonance and to EIT-like resonant peak, but the resonant wavelengths are kept constant and located at 1548.06 nm and 1548.23 nm. When the distance gap d is large, such as $d = 1.8$ μm and 1.5 μm in Fig. 2, the normalized background intensity to the intensity without coupling between fiber taper and microcavity is 0.944 and 0.813, with only 0.2 dB and 0.9 dB insertion loss due to weak coupling strength respectively. The background amplitude is much larger than the discrete resonant mode, which leads to the resonant dip. These transmission spectra are similar to the typical results in the previous experiments with large fiber taper. The Q factor of these resonant modes can be up to $\sim 10^6$ in this undercoupling condition.

As fiber taper moves closer to the cylindrical cavity, the coupling strength becomes stronger. More energy transfers from fiber taper to the radiation mode of the cylinder due to large coupling strength, which brings large coupling loss. Together with other losses, the total insertion loss of the coupling system becomes relatively large and leads to the decline of background amplitude. As the distance gap decreases to 1.2 μm, 0.7 μm and 0.4 μm, the intensity of transmitted background declines with the loss of 2.0 dB, 4.7 dB and 8.2 dB, respectively. Meanwhile, the intensity of resonant mode changes with the varied coupling strength. When the amplitudes of resonant WGM coupled out of microcavity and transmitted background become comparable, they interfere with each other and Fano resonance with asymmetric lineshape is observed clearly ($d = 1.2$ μm, 0.7 μm, and 0.4 μm in Fig. 2). Ultimately, when the taper contacts with the microcavity ($d = 0$ μm), EIT-like resonant

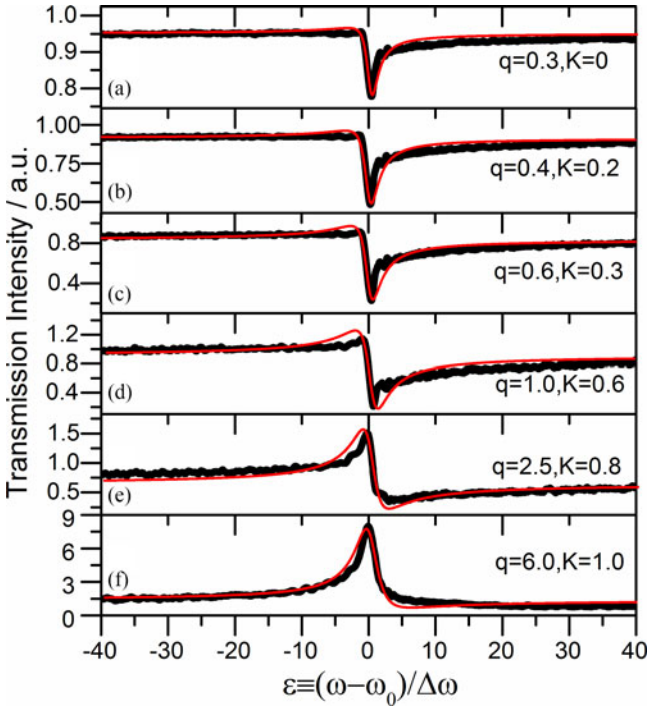

Fig. 3. Zoom-in transmission spectra in the vicinity of 1548.06 nm with different distance gap $d = 1.8\ \mu$m (a), 1.5 μm (b), 1.2 μm (c), 0.7 μm (d), 0.4 μm (e), and 0 μm (f). All traces are normalized to the intensity of individual continuous backgrounds. $\varepsilon \equiv (\omega - \omega_0)/\Delta\omega$ is the normalized frequency detuning. The black and red traces are the experimental and theoretical results, respectively.

peak occurs and its Q factor decreases to $\sim 3 \times 10^5$. In this condition, most energy of input light is transferred to the delocalized radiation mode, and severe insertion loss of 15.3 dB leads to dramatic decrease of the background intensity, nearly to zero. The discrete resonant amplitude is much larger than the background amplitude and EIT-like resonant peak occurs in the transmission spectrum.

In order to study the whole evolution of Fano resonance in detail, Fig. 3 focuses on the dynamic Fano lineshape at the resonant wavelength 1548.06 nm. The experimental traces fit well with the theoretical model of Fano resonance as follows [2], [16]:

$$I(\omega) = \frac{|q - \varepsilon - iK|^2}{(1+K)^2 + \varepsilon^2} \tag{1}$$

where q is the Fano parameter, denoting the ratio of discrete resonant amplitude to the transmitted background amplitude. $\varepsilon \equiv (\omega - \omega_0)/\Delta\omega$ is the frequency detuning between incident light ω and resonant frequency ω_0; here, $\Delta\omega$ is the spectral width of Fano resonance. K is the ratio of modified decay rate to coupling strength.

According to Formula (1), the dominant factor accounting for the lineshape evolution is Fano parameter, which characterizes the degree of asymmetry. In our particular case, the q parameter is defined as ratio of the amplitude of WGM coupled out of microcavity to the directly transmitted background. Experimentally, as the coupling position is moved close to the microcavity, Fano parameter gradually increases with the decrease of distance gap. The lineshape of the transmission spectrum transforms from resonant dip to asymmetrical Fano resonance and ultimately to EIT-like resonant peak. The lineshape is dynamically adjusted through changing Fano parameter by tuning the gap. When the distance gap is large as $d = 1.8\ \mu$m and 1.5 μm (in Fig. 3(a) and (b)), the Fano parameter is relatively low and the transmission spectrum appears quasi-Lorentz lineshape. As the distance gap decreases to 1.2 μm, the Fano parameter increases to 0.6 and asymmetrical

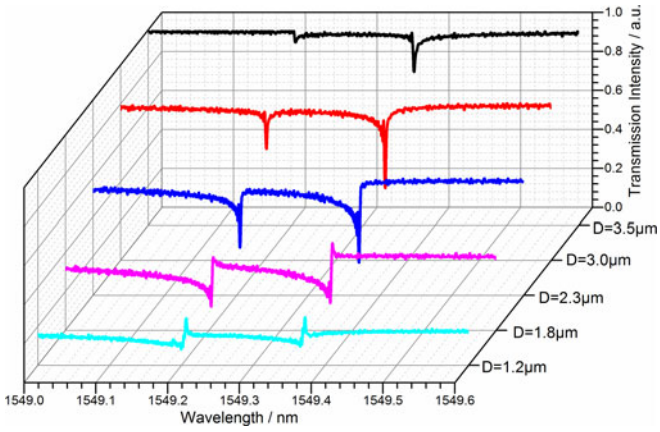

Fig. 4. Transmission spectra with various coupling diameter D of fiber taper.

lineshape begins to occur. Further decreasing the gap to 0.7 μm, typical asymmetrical Fano lineshape is observed at $q = 1$, where the amplitude of discrete resonant WGM equals the transmitted background. As distance gap decreases to 0.4 μm, the Fano parameter increases to 2.5 and the degree of asymmetry of Fano resonance becomes more obvious. Ultimately, when the fiber taper is in touch with the cylindrical microcavity, the Fano parameter increases to 6 and EIT-like lineshape occurs because the amplitude of resonant mode is much larger than the background due to severe insertion loss. Thus, by adjusting the gap between fiber taper and cylindrical microcavity, different lineshapes of Fano resonance can be simply achieved through decreasing the background intensity to be comparable to the resonant WGM intensity.

In additions, by adjusting the coupling diameter D of the fiber taper, we also observe the similar evolution of Fano resonance in fiber taper coupled microcylinder, shown in Fig. 4. In the experiment, we change the coupling diameter D of the taper through moving fiber taper along its axis. Throughout the manipulation process, the fiber taper keeps in touch with cylindrical microcavity. When the coupling diameter of fiber taper is large ($D = 3.5$ μm and 3 μm), the coupling process suffers from little insertion loss and no obvious Fano lineshape (black and red traces in Fig. 4) is observed due to the relatively large background intensity. This is because the coupling taper has large mode index, so little energy of input light is coupled to radiation mode. With the decrease of coupling diameter to $D = 2.3$ μm and 1.8 μm, the insertion loss becomes larger and is mainly dominated by coupling loss to radiation mode. Then the amplitude of transmitted background becomes weak to be comparable to that of WGM. Obvious Fano lineshapes (blue and magenta traces in Fig. 4) are generated and the lineshape is dynamically evolved due to the variation of Fano parameter. Ultimately, EIT-like lineshape (cyan trace in Fig. 4) exists in the transmission spectrum as the coupling position is located at the smallest diameter of the taper ($D = 1.2$ μm). It should be noted that the resonant wavelengths are kept almost constant at the different coupling diameters. If the diameter of the fiber taper continues to decrease (less than 1 μm), mode index of fiber taper is smaller and higher order modes can be generated due to the phase matching. Meanwhile, more energy turns into radiation modes and the insertion loss will be much larger. The intensity of resonant peaks and background will continue to decline.

In order to demonstrate the unique property of cylindrical microcavity, we replace the microcylinder with microsphere, but use the same thin fiber taper with $\sim$1 μm diameter. As we dynamically adjust the distance gap between fiber taper and microsphere from the undercoupling to the overcoupling, no obvious Fano resonance but the typical resonant dip is observed within all the manipulation processes. The biggest difference in the transmission spectrum is the depth of the WGM resonant dip, which origins from the variation of coupling strength [22]. In the whole manipulation process, the background intensity of thin fiber taper coupled microsphere experiences little insertion loss, i.e., less than 1 dB, even when thin taper contacts with the microsphere, which is much lower than

cylindrical microcavity in the same condition. The intensity of discrete resonant WGM is always much smaller than the background, and therefore, no obvious asymmetric lineshape is observed in the whole evolution process. The principal difference between microcylinder and microsphere is that the microcylinder possesses the additional delocalized modes.

3. Conclusion

In conclusion, the combination of thin fiber taper and cylindrical microcavity provides an easy and efficient method to excite Fano resonance. The discrete WGM and weak continuous background interfere with each other in the fiber taper to generate Fano resonance. We experimentally observe the Fano resonance evolving from resonant dip to asymmetrical Fano lineshape, and to EIT-like resonant peak ultimately in fiber taper coupled cylindrical microcavity, by changing the distance gap between fiber taper and cylindrical microcavity or varying the coupling diameter of fiber taper. The experimental results agree well with the theoretical prediction. Meanwhile, we also demonstrate the unique property of microcylinder for Fano resonance. The whole experimental system in our paper provides a platform for optics filter, biochemical sensing based on Fano-type resonance.

References

[1] S. J. Yong, M. S. Arkady, and K. Chang Sub, "Classical analogy of Fano resonances," *Physica Scripta*, vol. 74, 2006, Art. no. 259.
[2] U. Fano, "Effects of configuration interaction on intensities and phase shifts," *Phys. Rev.*, vol. 124, pp. 1866–1878, Dec. 15, 1961.
[3] B.-B. Li *et al.*, "Experimental controlling of Fano resonance in indirectly coupled whispering-gallery microresonators," *Appl. Phys. Lett.*, vol. 100, 2012, Art. no. 021108.
[4] H.-T. Lee and A. W. Poon, "Fano resonances in prism-coupled square micropillars," *Opt. Lett.*, vol. 29, pp. 5–7, Jan. 1, 2004.
[5] S. Fan, "Sharp asymmetric line shapes in side-coupled waveguide-cavity systems," *Appl. Phys. Lett.*, vol. 80, pp. 908–910, 2002.
[6] Y.-F. Xiao, M. Li, Y.-C. Liu, Y. Li, X. Sun, and Q. Gong, "Asymmetric Fano resonance analysis in indirectly coupled microresonators," *Phys. Rev. A*, vol. 82, Dec. 29, 2010, Art. no. 065804.
[7] M. Asano *et al.*, "Controlling slow and fast light and dynamic pulse-splitting with tunable optical gain in a whispering-gallery-mode microcavity," *Appl. Phys. Lett.*, vol. 108, 2016, Art. no. 181105.
[8] J. Liao, X. Wu, L. Liu, and L. Xu, "Fano resonance and improved sensing performance in a spectral-simplified optofluidic micro-bubble resonator by introducing selective modal losses," *Opt. Exp.*, vol. 24, pp. 8574–8580, Apr. 18, 2016.
[9] E. Semouchkina, R. Duan, G. Semouchkin, and R. Pandey, "Sensing based on Fano-type resonance response of all-dielectric metamaterials," *Sensors*, vol. 15, pp. 9344–9359, 2015.
[10] P. Fan, Z. Yu, S. Fan, and M. L. Brongersma, "Optical Fano resonance of an individual semiconductor nanostructure," *Nature Mater.*, vol. 13, pp. 471–475, 2014.
[11] B. Luk'yanchuk *et al.*, "The Fano resonance in plasmonic nanostructures and metamaterials," *Nature Mater.*, vol. 9, pp. 707–715, 2010.
[12] F. Lei, B. Peng, Ş. K. Özdemir, G. L. Long, and L. Yang, "Dynamic Fano-like resonances in erbium-doped whispering-gallery-mode microresonators," *Appl. Phys. Lett.*, vol. 105, 2014, Art. no. 101112.
[13] A. Chiba, H. Fujiwara, J.-I. Hotta, S. Takeuchi, and K. Sasaki, "Fano resonance in a multimode tapered fiber coupled with a microspherical cavity," *Appl. Phys. Lett.*, vol. 86, 2005, Art. no. 261106.
[14] K. J. Vahala, "Optical microcavities," *Nature*, vol. 424, pp. 839–846, 2003.
[15] B.-B. Li *et al.*, "Experimental observation of Fano resonance in a single whispering-gallery microresonator," *Appl. Phys. Lett.*, vol. 98, 2011, Art. no. 021116.
[16] Y.-F. Xiao *et al.*, "Tunneling-induced transparency in a chaotic microcavity," *Laser Photon. Rev.*, vol. 7, pp. L51–L54, 2013.
[17] L. Wang, D. Lippolis, Z.-Y. Li, X.-F. Jiang, Q. Gong, and Y.-F. Xiao, "Statistics of chaotic resonances in an optical microcavity," *Phys. Rev. E*, vol. 93, Apr. 4, 2016, Art. no. 040201.
[18] B. Peng, Ş. K. Özdemir, W. Chen, F. Nori, and L. Yang, "What is and what is not electromagnetically induced transparency in whispering-gallery microcavities," *Nature Commun.*, vol. 5, 2014, Art. no. 5082.
[19] M. Sumetsky, "Mode localization and the Q-factor of a cylindrical microresonator," *Opt. Lett.*, vol. 35, pp. 2385–2387, Jul. 15, 2010.
[20] A. W. Poon, R. K. Chang, and J. A. Lock, "Spiral morphology-dependent resonances in an optical fiber: Effects of fiber tilt and focused Gaussian beam illumination," *Opt. Lett.*, vol. 23, pp. 1105–1107, Jul. 15, 1998.
[21] J. C. Knight, G. Cheung, F. Jacques, and T. A. Birks, "Phase-matched excitation of whispering-gallery-mode resonances by a fiber taper," *Opt. Lett.*, vol. 22, pp. 1129–1131, Aug. 1, 1997.
[22] M. Cai, O. Painter, and K. J. Vahala, "Observation of critical coupling in a fiber taper to a silica-microsphere whispering-gallery mode system," *Phys. Rev. Lett.*, vol. 85, pp. 74–77, Jul. 3, 2000.